# High-temperature phases of multiferroic $BiFe_{0.7}Mn_{0.3}O_3$

Alexandra S. Gibbs,[1,2] Donna C. Arnold,[1,3] Kevin S. Knight,[4] and Philip Lightfoot[1,*]

[1]*School of Chemistry and EaStCHEM, University of St Andrews, North Haugh, St Andrews KY16 9ST, Scotland, United Kingdom*

[2]*Scottish Universities Physics Alliance, School of Physics and Astronomy, University of St Andrews, North Haugh, St Andrews KY16 9SS, Scotland, United Kingdom*

[3]*School of Physical Sciences, University of Kent, Canterbury, Kent CT2 7NH, England, United Kingdom*

[4]*ISIS Facility, Rutherford Appleton Laboratory, Chilton, Didcot OX11 OQX, England, United Kingdom*

(Received 16 April 2013; revised manuscript received 10 May 2013; published 17 June 2013)

We report the results of a high-resolution powder neutron-diffraction study of multiferroic $BiFe_{0.7}Mn_{0.3}O_3$. We have confirmed the previous assignment of the $\alpha$ phase and $\beta$ phase as having $R3c$ and $Pbnm$ symmetry, respectively. The $\gamma$ phase, however, has been shown unequivocally not to be cubic, as previously reported, but rather to retain octahedral tilting distortions leading to a lower symmetry, most likely rhombohedral with space group $R\bar{3}c$. The $\gamma$ phase of $BiFe_{0.7}Mn_{0.3}O_3$ is therefore different than that of the parent compound $BiFeO_3$, which retains an orthorhombic structure up to its decomposition temperature. The lattice parameters of the $\gamma$ phase of $BiFe_{0.7}Mn_{0.3}O_3$ are pseudocubic throughout its entire stability range, despite the fact that there are still significant distortions from the cubic aristotype structure even at the onset of decomposition.

DOI: 10.1103/PhysRevB.87.224109 PACS number(s): 61.05.fm, 61.50.Ks, 75.85.+t

## I. INTRODUCTION

$BiFeO_3$ is one of the most well studied of the multiferroic materials, partly due to the fact that it is in the multiferroic state at room temperature with coexisting antiferromagnetic and ferroelectric orders. Despite this, the details of its high-temperature phase transitions have only recently been resolved,[1,2] and the details of its low-temperature structural and magnetic properties are still debated. The pure compound has three structural phases at and above room temperature. The ferroelectric $\alpha$ phase, which is multiferroic below $T_N = 643$ K, has the space group $R3c$ (although recent work has suggested a very subtle monoclinic[3] or even triclinic[4] distortion) and is stable from low temperature up to $T_{\alpha-\beta} = 1093$ K. The orthorhombic $\beta$ phase with space group $Pbnm$ (a nonstandard setting of $Pnma$) is stable up to $T_{\beta-\gamma} = 1198$ K,[1] and the $\gamma$ phase exists in the small window between $T_{\beta-\gamma}$ and the decomposition temperature of 1223 K.[2]

Many dopants have been used to modify or stabilize the properties of $BiFeO_3$ and also to try to gain insight into the underlying physics of the undoped parent compound.[5–7] Substitution of $Mn^{3+}$ for $Fe^{3+}$ increases the magnetization and dielectric constant, although $T_N$ and $T_C$ are lower than in the pure compound.[5,8,9] The Mn-substituted compound $BiFe_{0.7}Mn_{0.3}O_3$ has been reported, based upon x-ray diffraction, differential thermal analysis (DTA), dilatometry, and conductivity data, to have lower transition temperatures than the parent compound: $T_{\alpha-\beta} = 943$ K and $T_{\beta-\gamma} = 1160$ K, with peritectic decomposition reported at 1193 K.[10,11] The Néel temperature is also decreased to $T_N = 533$ K. $BiFe_{0.7}Mn_{0.3}O_3$, when prepared at ambient pressure, is reported to adopt the same $\alpha$ and $\beta$ phases as the parent $BiFeO_3$; however, the $\gamma$ phase has been reported to be cubic, unlike the parent compound, with the aristotype $Pm\bar{3}m$ structure.[10,11] Under high-pressure synthesis conditions a different, $PbZrO_3$-like, orthorhombic form is stabilized at ambient temperature.[12,13] The $\gamma$ phase of $BiFeO_3$ has been reported to be metallic,[14] whereas the $\beta$ and $\gamma$ phases of $BiFe_{0.7}Mn_{0.3}O_3$ are semiconducting.[11] Both the $\alpha$-to-$\beta$ and $\beta$-to-$\gamma$ transitions of $BiFe_{0.7}Mn_{0.3}O_3$ were confirmed to be first order in nature by DTA.[10,11]

Since the only diffraction studies of the high-temperature phases so far have used x-ray powder diffraction, a neutron-diffraction experiment was carried out to determine whether the increased sensitivity of the technique to oxygen atom positions could shed any further light on the high-temperature phases of $BiFe_{0.7}Mn_{0.3}O_3$.

## II. EXPERIMENTAL

### A. Sample synthesis and characterization

Samples of $BiFe_{0.7}Mn_{0.3}O_3$ were synthesized by the rapid liquid phase sintering technique. This method has been used previously for both pure $BiFeO_3$ and $BiFe_{0.7}Mn_{0.3}O_3$, as the liquid $Bi_2O_3$ at the sintering temperature ensures quick reaction, which reduces loss of volatile $Bi_2O_3$ and impurity phases due to the metastability of $BiFeO_3$ and $BiFe_{0.7}Mn_{0.3}O_3$ toward mullite- and sillenite-type compounds $Bi_2Fe_{4-x}Mn_xO_9$ and $Bi_{25}Fe_{1-y}Mn_yO_{39}$ at the sintering temperature. The appropriate ratios of the reactant oxide powders $Bi_2O_3$, $Fe_2O_3$, and $Mn_2O_3$ were mixed and acetone ground to ensure small particle size and thorough mixing. The powder was then compressed into small pellets and sintered in a preheated furnace at 1173 K for 10 min followed by quenching in air to room temperature. Previous reports by Selbach *et al.* have found that this preparation method (quenching in air from 1173 K) results in samples of $BiFe_{0.7}Mn_{0.3}O_{3+\delta}$ with $\delta = 0.030 \pm 0.005$.[10,11] No separate analysis of the oxygen nonstoichiometry was performed by us. During the Rietveld refinements of the neutron powder-diffraction data, refinement of the cation site occupancies gave a variation of less than 1.5% and no detectable improvement in the fit.

### B. Powder neutron diffraction

Powder neutron-diffraction experiments were carried out on the high-resolution powder diffractometer (HRPD) at ISIS. The samples were sealed in an evacuated quartz tube and placed in a vanadium can, which was then mounted in a standard Rutherford Appleton Laboratory furnace. Data were

 

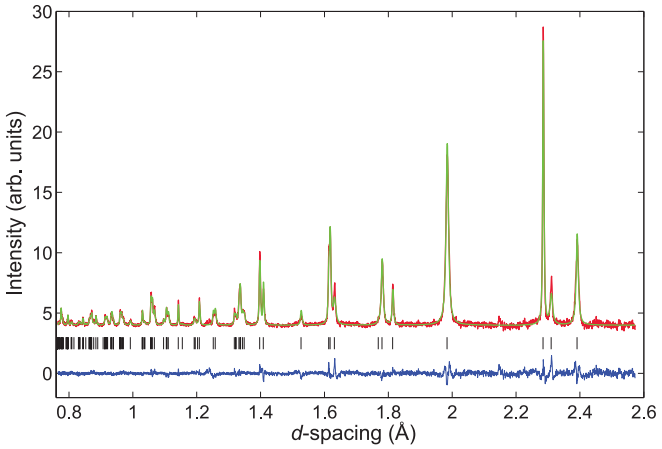


FIG. 1. (Color online) The Rietveld refinement for the 523-K data set with space group $R3c$ including anisotropic broadening. The observed data points are plotted in red, the calculated profile is plotted in green, and the difference profile is plotted in blue. The black ticks mark the expected reflection positions for the $R3c$ space group. The small additional peaks, for example at 2.15 Å, are from the vanadium sample can.

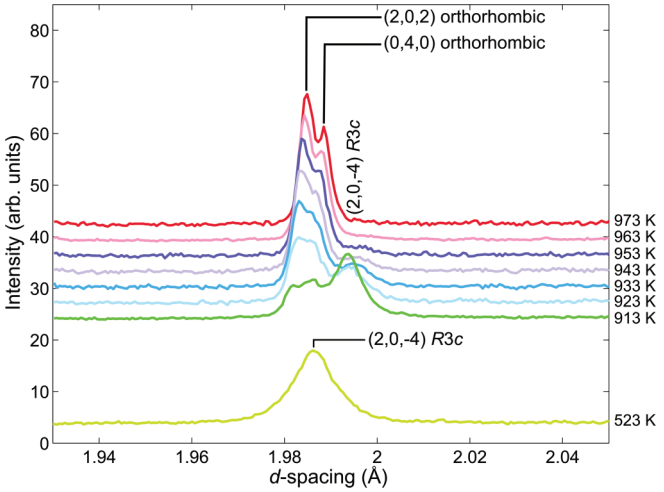


FIG. 2. (Color online) The diffraction patterns taken across the $\alpha$-to-$\beta$ transition of $BiFe_{0.7}Mn_{0.3}O_3$. There is coexistence of the rhombohedral and orthorhombic phases between 913 and 953 K. The transition is complete by 963 K as evidenced by the disappearance of the (2,0,−4) peak.

taken at 44 temperatures between room temperature and 1191 K. Appropriate equilibration times were included upon each temperature change. In the $\beta$ phase, short data collection times, corresponding to a 15-$\mu$A h incident proton beam, were used for most runs to ensure that in the metastable region transformations to the mullite and sillenite phases were minimized. These were interspersed with longer runs of 50 $\mu$A h at 913, 963, 1013, 1113, and 1153 K. In the $\gamma$ phase, 30-$\mu$A h exposures were recorded per data set up to 1173 K and 8 $\mu$A h at each temperature above except for at 1173 K, where 50 $\mu$A h was collected, and 1191 K, where 10 $\mu$A h was collected.

The data used for analysis were taken from the backscattering bank and additionally from the 90° bank for analysis of the $\beta$ phase. Data were refined using the Rietveld method as implemented in the general structure analysis system (GSAS).[15]

## III. RESULTS

The room-temperature diffraction patterns confirmed the phase purity of the sample, with no additional peaks observed beyond those belonging to vanadium from the sample can. The previous assignment by Selbach *et al.*[10,11] and Sosnowska *et al.*[16] of space group $R3c$ for the $\alpha$ phase was also confirmed, with no evidence of symmetry lowering as recently suggested for $BiFeO_3$. A substantial amount of anisotropic broadening was present, however, with a variation of more than a factor of 2 between the full width half maxima of some peaks (see supplemental material[17] for further details). A Rietveld refinement for the 523-K data set, including terms for anisotropic broadening, gave a satisfactory fit, as can be seen in Fig. 1. The results of the refinement are tabulated in Table I, and a crystallographic information file (CIF) is included in the supplemental material.[17] Due to the instrumental characteristics of HRPD, which is optimized for low-$d$-spacing structural studies, and the time-of-flight window used for the experiment (30–130 ms), detailed study of the magnetic structure was not possible. One pure magnetic reflection was observed below $T_N$ at 4.58 Å which could correspond to the (101/003) reflection observed by Sosnowska *et al.* for $BiFe_{0.8}Mn_{0.2}O_3$.[18]

### A. The α-to-β transition

The transition from the $\alpha$ phase to the $\beta$ phase is clear upon visual examination of the diffraction patterns. As can be seen in Fig. 2, the (2,0,−4) peak of the rhombohedral phase is not visible above 963 K.

TABLE I. The Rietveld refinement results of the $R3c$ model (including anisotropic broadening) for the $\alpha$ phase of $BiFe_{0.7}Mn_{0.3}O_3$ at 523 K. The lattice parameters are $a = 5.58833(16)$ Å and $c = 13.8588(5)$ Å. The Bi $z$ parameter was kept fixed during the refinement to define the origin of the polar axis. The refinement gave $R_{wp} = 0.0307$, $\chi^2 = 2.143$ for 41 variables. Further details of the refined variables can be found in the supplemental material.[17]

| Atom | Site | $x$ | $y$ | $z$ | $U_{iso}$ ×100 (Å$^2$) | Occ. |
|---|---|---|---|---|---|---|
| Bi | 6*a* | 0 | 0 | 0 | 1.94(7) | 1 |
| Fe | 6*a* | 0 | 0 | 0.22620(17) | 1.63(10) | 0.7 |
| Mn | 6*a* | 0 | 0 | 0.22620(17) | 1.63(10) | 0.3 |
| O | 18*b* | 0.4504(4) | 0.0180(4) | 0.95600(19) | 2.27(7) | 1 |

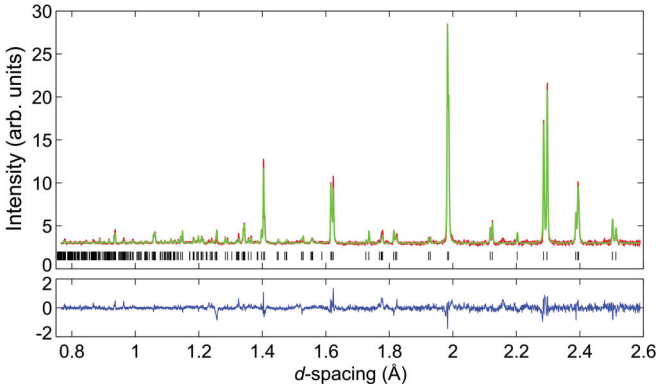


FIG. 3. (Color online) The Rietveld refinement results for the 963-K data in the $\beta$ phase of $BiFe_{0.7}Mn_{0.3}O_3$ in space group $Pnma$. The observed data points are plotted in red, the calculated profile is plotted in green, and the difference profile is plotted in blue. The black ticks mark the expected reflection positions for the $Pnma$ space group.

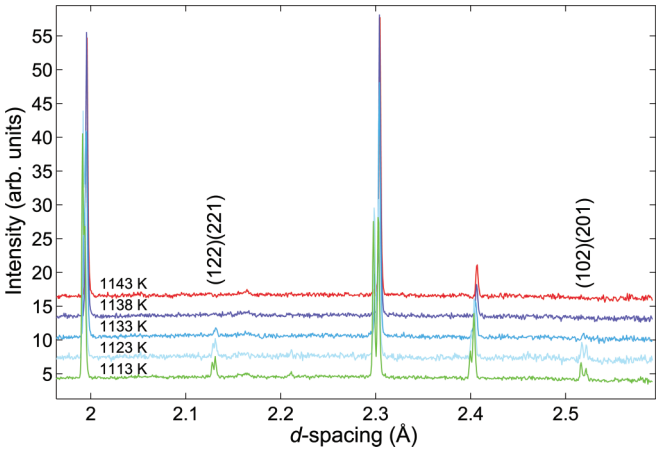


FIG. 4. (Color online) A range of the diffraction data across the $\beta$-to-$\gamma$ transition of $BiFe_{0.7}Mn_{0.3}O_3$. The labeled peaks, which disappear in the $\gamma$ phase, correspond to $M_3^+$-mode distortions. The small, broad peak just above $d = 2.15$ Å is from the vanadium sample can.

The previous assignment of $Pnma$ as the space group of the $\beta$ phase is confirmed by our data. In-depth investigation of other possible space groups based upon analysis of superlattice reflections of the perovskite aristotype structure[19,20] failed to find any model with a significantly better fit. This analysis relates distortions around different high-symmetry points in the Brillouin zone to fractional-index reflections of the $Pm\bar{3}m$ cubic aristotype structure. The distortions are labeled with the irreducible representation of the distortion mode. The relevant distortion modes of the $Pm\bar{3}m$ structure are $R_4^+$, $M_3^+$, $X_5^+$, and $\Gamma_4^-$. The superlattice reflections index as $(h,k,l)_{\text{parent}} \pm (\frac{1}{2},\frac{1}{2},\frac{1}{2})$ for $R_4^+$-mode distortions, $(h,k,l)_{\text{parent}} \pm (\frac{1}{2},0,\frac{1}{2})$ for $M_3^+$-point distortions, and $(h,k,l)_{\text{parent}} \pm (0,\frac{1}{2},0)$ for $X_5^+$-mode distortions. $\Gamma_4^-$-mode distortions do not produce superlattice peaks but instead modify the intensities of the aristotype peaks. Structurally the $R_4^+$-mode peaks correspond to out-of-phase tilts of adjacent octahedra, and the $M_3^+$-mode peaks correspond to analogous in-phase tilts. The $X_5^+$-mode peaks appear as a consequence of the presence of both $R_4^+$- and $M_3^+$-mode distortions. $\Gamma_4^-$-mode distortions are composed of polar cation displacements. The possible space groups for perovskites with combinations of these distortion modes have been tabulated (for simple distortions) by Howard and Stokes[21] and Stokes *et al.*[22] Four space groups are possible for concurrent $R_4^+$- and $M_3^+$-mode distortions, and a further twelve are possible for $R_4^+$-, $M_3^+$-, and $\Gamma_4^-$-mode distortions.[22] Of these 16 space groups 8 were ruled out by the diffraction pattern violating either lattice symmetry or centering conditions. Of the remaining eight a further four were ruled out by a lack of peak splitting necessitating such low symmetry. The remaining space groups were $Pnma$ and its polar subgroups $Pmn2_1$, $Pmc2_1$, and $Pna2_1$.

The $Pnma$ model (corresponding to Glazer notation $a^-b^+a^-$) gave a good fit with $R_{wp} = 0.0276$, $\chi^2 = 4.447$ for 69 variables. The results of the Rietveld refinement are shown in Fig. 3 and in Table II, and a crystallographic information file (CIF) is included in the supplemental material.[17] The polar subgroups of $Pnma$ gave satisfactory fits, as can be seen in the supplemental material.[17] Indeed, both $Pmc2_1$ and $Pmn2_1$ gave somewhat lower $R_{wp}$ and $\chi^2$ values than $Pnma$. However, under visual inspection the difference in the fits was very small (see supplemental material[17]). Comparisons of each of these models over the entire temperature range of the $\beta$ phase failed to show any significant improvement on lowering the symmetry. In the absence of a significant improvement over $Pnma$, and of any physical property measurements indicating the necessity of a polar space group, $Pnma$ was judged to be the most appropriate space group for the $\beta$ phase of $BiFe_{0.7}Mn_{0.3}O_3$.

We have therefore confirmed that, in agreement with previous reports,[10,23] the $\alpha$ and $\beta$ phases of $BiFe_{0.7}Mn_{0.3}O_3$ are isostructural to those of pure $BiFeO_3$, adopting space groups $R3c$ and $Pnma$, respectively.

TABLE II. The Rietveld refinement results of the $Pnma$ model for the $\beta$ phase at 963 K. The lattice parameters are $a = 5.62738(14)$ Å, $b = 7.94594(18)$ Å, and $c = 5.58786(14)$ Å. The refinement gave $R_{wp}$(bank 1) = 0.0276, $R_{wp}$(bank 2) = 0.0264, $\chi^2 = 4.447$ for 69 variables.

| Atom | Site | $x$ | $y$ | $z$ | $U_{\text{iso}}$ ×100 (Å$^2$) | Occ. |
|---|---|---|---|---|---|---|
| Bi | 4$c$ | 0.9773(4) | 0.25 | 0.5033(4) | 8.34(9) | 1 |
| Fe | 4$a$ | 0 | 0 | 0 | 4.16(9) | 0.7 |
| Mn | 4$a$ | 0 | 0 | 0 | 4.16(9) | 0.3 |
| O1 | 4$c$ | 0.0165(5) | 0.25 | 0.0660(4) | 6.06(11) | 1 |
| O2 | 8$d$ | 0.2902(3) | 0.9634(2) | 0.2088(3) | 7.68(11) | 1 |

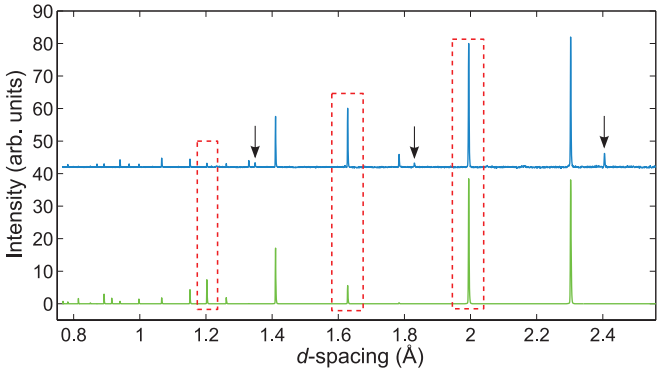


FIG. 5. (Color online) The predicted pattern for the cubic aristotype $Pm\bar{3}m$ structure (lower, green) and the diffraction pattern for $T = 1153$ K in the $\gamma$ phase (upper, blue). The arrows mark the peaks due to $R_4^+$-mode distortions. The red dotted boxes indicate peaks for which the the observed intensities differ strongly relative to those predicted for the cubic aristotype structure.

### B. The $\beta$-to-$\gamma$ transition

Due to the isostructural nature of $BiFe_{0.7}Mn_{0.3}O_3$ and $BiFeO_3$ in the $\alpha$ phase and $\beta$ phases it might be expected that the $\gamma$ phases would also be isostructural. Selbach *et al.*, however, have previously reported the $\gamma$ phase of $BiFe_{0.7}Mn_{0.3}O_3$ to adopt the perovskite aristotype cubic structure (space group $Pm\bar{3}m$) based upon x-ray powder-diffraction data.[11]

The transition to the $\gamma$ phase is clear in our diffraction data, as can be seen in Fig. 4. There is a disappearance of $M_3^+$- and $X_5^+$-mode peaks which also correspond to body-centred systematic absences for the same orthorhombic unit cell, at and above 1138 K. This is in clear contrast to the parent compound $BiFeO_3$, which retains an orthorhombic structure up to its decomposition point.

Additionally, it is also clear that the $\gamma$ phase of $BiFe_{0.7}Mn_{0.3}O_3$ is *not* cubic. This is shown by the continued presence of $R_4^+$-mode distortion peaks, as shown in Fig. 5 (arrows). The presence of these peaks gives, from the analysis

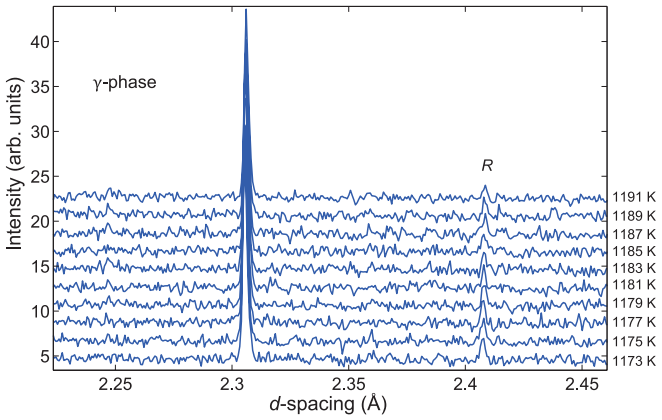


FIG. 6. (Color online) The highest-temperature data taken in the $\gamma$ phase of $BiFe_{0.7}Mn_{0.3}O_3$. The label $R$ indicates one of the $R_4^+$-mode peaks still present at the highest temperature measured. As the sample was beginning to decompose at the highest temperature with no indication of a phase transition, it seems that the aristotype cubic phase is not reached within the stability range of $BiFe_{0.7}Mn_{0.3}O_3$.

TABLE III. The $R_{wp}$, $\chi^2$, and oxygen atom $U_{iso}$ values for the fully isotropic $R\bar{3}c$, $I4/mcm$, and $Imma$ refinements for the $\gamma$ phase at 1153 K.

| Space group | $R_{wp}$ | $\chi^2$ | Oxygen site $100 \times U_{iso}$ (Å$^2$) |
|---|---|---|---|
| $I4/mcm$ | 0.0319 | 3.365 (36 var.) | O1: 37.7(17) |
| | | | O2: 5.84(18) |
| $Imma$ | 0.0327 | 3.535 (36 var.) | O1: 6.9(3) |
| | | | O2: 11.5(3) |
| $R\bar{3}c$ | 0.0362 | 4.331 (33 var.) | O1: 7.88(12) |

of Stokes *et al.*[22] (based upon simple tilt systems), the possible space groups $I4/mcm$, $Imma$, $R\bar{3}c$, $C2/m$, $C2/c$, and $P\bar{1}$ corresponding to Glazer tilt systems $a^0a^0c^-$, $a^0b^-b^-$, $a^-a^-a^-$, $a^0b^-c^-$, $a^-a^-c^-$, and $a^-b^-c^-$). Although the symmetry is clearly lower than cubic, the lattice parameters are metrically cubic within experimental error for all data sets in the $\gamma$ phase.

It can also be seen in Fig. 5 that the intensities of the aristotype reflections differ substantially from those expected (unlike the $\beta$ phase). This could be due to either strongly anisotropic atomic displacement parameters or activity of polar $\Gamma_4^-$-mode distortions.

Inspection of the highest-temperature data, shown in Fig. 6, gives no sign of a further phase transition with $R$-point distortion peaks visible up to the highest temperatures measured where signs of decomposition became evident.

To identify the space group of the $\gamma$ phase, refinements of all of the candidate space-group models were undertaken. Monoclinic and triclinic space groups were ruled out due to a lack of any splitting of the extremely narrow peaks which would necessitate such a low-symmetry structure. The remaining three space groups, $I4/mcm$, $Imma$, and $R\bar{3}c$, correspond to the presence of equal adjacent out-of-phase tilts along one, two, or three axes, respectively.

The tetragonal space group $I4/mcm$ could be ruled out by the unphysical $U_{iso}$ values produced by the refinement. The inclusion of anisotropic thermal displacement parameters did not improve the fit and again resulted in physically unreasonable values.

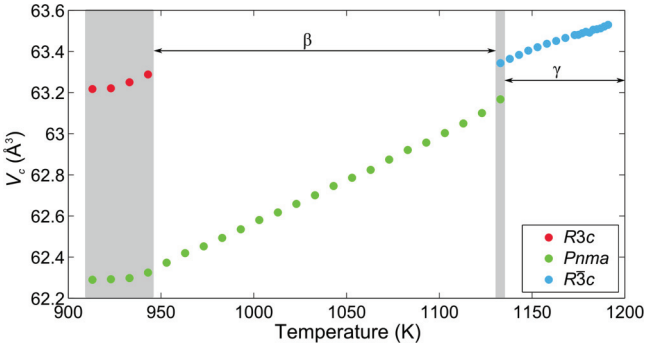


FIG. 7. (Color online) The normalized unit-cell volumes for the high-temperature phases of $BiFe_{0.7}Mn_{0.3}O_3$. The volumes plotted are normalized per formula unit for all phases. The areas shaded gray indicate phase coexistence.

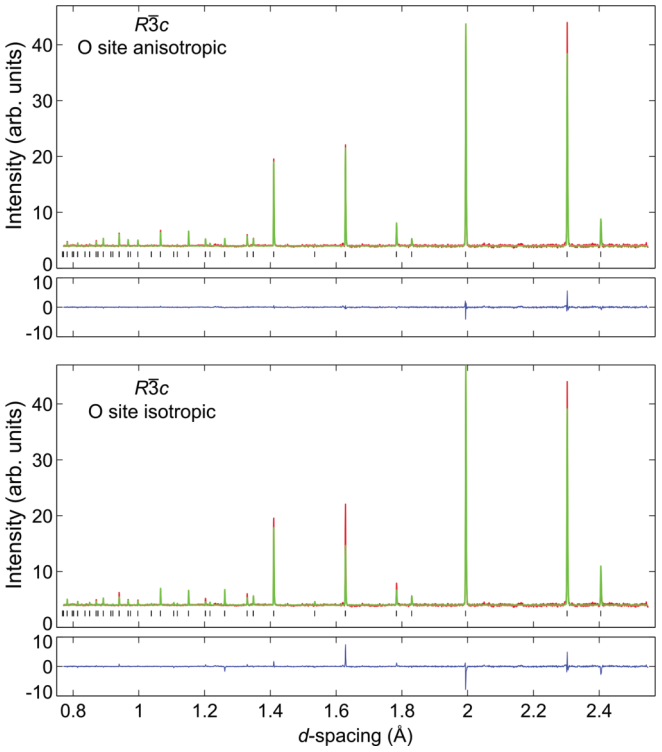


FIG. 8. (Color online) The results of the Rietveld refinements of the $R\bar{3}c$ model for the $\gamma$ phase of $BiFe_{0.7}Mn_{0.3}O_3$ at 1153 K. The observed data points are plotted in red, the calculated profile is plotted in green, and the difference profile is plotted in blue. The black ticks mark the expected reflection positions for the $R3c$ space group. The upper panel shows the results of the refinement with anisotropic atomic displacement parameters for the oxygen site, and the lower panel shows the results from all sites treated isotropically.

The best fits with physically reasonable parameters were given by the $Imma$ and $R\bar{3}c$ models. Both of these space groups gave good fits with no peaks unindexed. The atomic displacement parameters were rather large for both space groups but not unreasonable, as can be seen in Table III . The atomic displacement parameter for the single oxygen site in the $R\bar{3}c$ refinement is smaller than for the equatorial O2 site in the $Imma$ model. Due to this, and also the fact that $R\bar{3}c$ is a higher-symmetry structure than $Imma$, we conclude that space group $R\bar{3}c$ provides the best model for the $\gamma$ phase of $BiFe_{0.7}Mn_{0.3}O_3$. This choice is supported further by carrying out comparative anisotropic refinements for these two space groups. The most significant improvements were found by

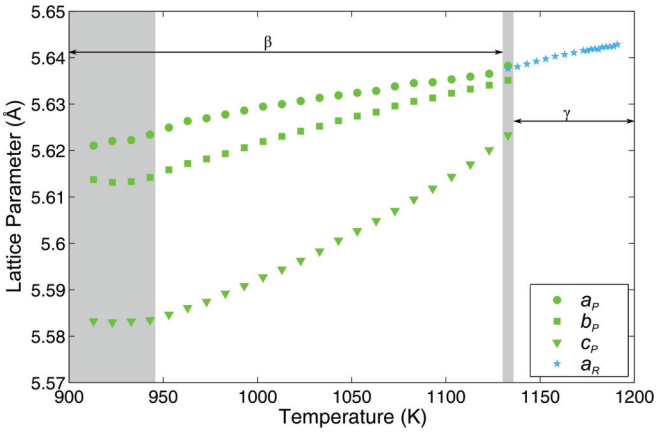


FIG. 9. (Color online) The lattice parameters for the $\beta$ and $\gamma$ phases of $BiFe_{0.7}Mn_{0.3}O_3$. The lattice parameters from the $\beta$ phase ($a_P$, $b_p$, and $c_p$) are those of the $Pnma$ unit cell, and for the $\gamma$ phase the rhombohedral parameter $a_R$ is used. This refers to the lattice parameters extracted from refinements in $R\bar{3}c$, since the lattice parameters are metrically cubic over the whole $\gamma$ phase $a_R = \sqrt{2}[c_R/(2\sqrt{3})]$. The areas shaded gray indicate phase coexistence.

allowing the O atoms to refine anisotropically, leading to $R_{wp}$ and $\chi^2$ values of $R_{wp} = 0.0218$, $\chi^2 = 1.572$ for 42 variables and $R_{wp} = 0.0222$, $\chi^2 = 1.634$ for 38 variables for the $Imma$ and $R\bar{3}c$ models, respectively.

The choice of $R\bar{3}c$ over $Imma$ is also indirectly supported by the first-order nature of the $\beta$-to-$\gamma$ transition, as seen in the discontinuity in the unit-cell volume. To allow ease of visualization of the unit-cell volume throughout the temperature-dependent phase diagram these were normalized to those of the pseudocubic unit cell, corresponding to the perovskite aristotype cell (thus allowing comparison of volumes for unit cells with equal numbers of formula units). The resulting trend in $V_c$ is shown in Fig. 7. This trend across the phase diagram is in general agreement with that reported by Selbach *et al.*[10,11] with a decrease in volume across the $\alpha$-to-$\beta$ transition and an increase across the $\beta$-to-$\gamma$ transition. The abrupt volume changes are consistent with the first-order nature of both transitions. With respect to the $\beta$-to-$\gamma$ transition, this clear evidence of the first-order nature points toward the correct space group for the $\gamma$ phase being $R\bar{3}c$ rather than $Imma$, as the transition $Pnma$-$R\bar{3}c$ must be first order by Landau theory[21] and is accompanied by a clear volume discontinuity in systems such as $LaGaO_3$.[24,25] The transition $Pnma$-$Imma$, however, is allowed to be second order by Landau theory, and in other perovskite systems such

TABLE IV. The Rietveld refinement results of the $R\bar{3}c$ isotropic model for the $\gamma$ phase at 1153 K. The lattice parameters are $a = 5.63969(19)$ Å, $c = 13.8146(8)$ Å. The refinement gave $R_{wp} = 0.0362$, $\chi^2 = 4.331$ for 33 variables. The results for the anisotropic model can be seen in the supplemental information.

| Atom | Wyckoff position | $x$ | $y$ | $z$ | $100 \times U_{iso}$ (Å$^2$) | Occ. |
|---|---|---|---|---|---|---|
| Bi | 6*a* | 0 | 0 | 0.25 | 7.81(11) | 1 |
| Fe | 6*b* | 0 | 0 | 0.5 | 1.23(6) | 0.7 |
| Mn | 6*b* | 0 | 0 | 0.5 | 1.23(6) | 0.3 |
| O | 18*e* | 0.4585(5) | 0 | 0.25 | 7.88(12) | 1 |

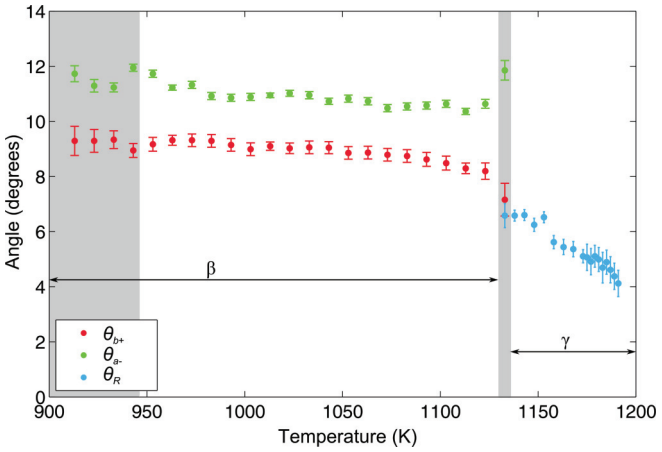


FIG. 10. (Color online) The octahedral tilt angles, as calculated by the method of Kennedy *et al.*,[27] for the $\beta$ and $\gamma$ phases of $BiFe_{0.7}Mn_{0.3}O_3$. The tilt angle is only expected to go to zero for temperatures above $T = 1200$ K. The areas shaded gray indicate phase coexistence.

as $SrRuO_3$ this transition shows no clear discontinuity in volume.[26] Although not conclusive, the clear discontinuity in volume across the $\beta$-to-$\gamma$ transition indicates, in agreement with the crystallographic evidence, that $R\bar{3}c$ is the most likely space group for the $\gamma$ phase of $BiFe_{0.7}Mn_{0.3}O_3$.

Comparative results of two Rietveld refinements of the $R\bar{3}c$ model, respectively, with fully isotropic atomic displacement parameters and with the oxygen site only refined anisotropically are shown in Fig. 8. The results of the fully isotropic refinement are tabulated in Table IV. The results of the anisotropic refinement and a crystallographic information file (CIF) for the isotropically refined structure are included in the supplemental material.[17] Investigation of anisotropic refinement of the Bi site gave no significant deviation from an isotropic ellipsoid and no clear improvement to the quality of the fits.

Figure 9 shows the lattice parameters of the $\beta$ and $\gamma$ phases, with the $R\bar{3}c$ model being used for the $\gamma$ phase. The lattice parameters increase smoothly throughout the $\beta$ and $\gamma$ phases. Interestingly, as previously mentioned, the lattice parameters are metrically cubic throughout the $\gamma$ phase.

Figure 10 shows the temperature dependence of the octahedral tilt angles through the $\beta$ and $\gamma$ phases. The tilt angle decrease with increasing temperature is consistent with the unit-cell expansion seen in Fig. 9, but this will also have a contribution from bond expansion effects. The abrupt decrease in the average tilt angle at the beta-gamma transition apparently leads to the increase in unit-cell volume observed at this point (Fig. 7); this behavior contrasts with the unit-cell volume decrease seen in $BiFeO_3$ itself at this point, previously ascribed to an insulator-metal transition.[2]

The trend of the tilt angle at highest temperatures furthermore indicates that the tilt angle would not be expected to go to zero until above $T = 1200$ K. This therefore confirms that a cubic phase of $BiFe_{0.7}Mn_{0.3}O_3$ is not realized within its stability range.

## IV. CONCLUSIONS

In conclusion, we have confirmed the previous assignments of the $\alpha$ and $\beta$ phases of $BiFe_{0.7}Mn_{0.3}O_3$ as rhombohedral (space group $R3c$) and orthorhombic (space group $Pnma$), respectively. However, we have shown conclusively that the previous assignment of cubic $Pm\bar{3}m$ for the $\gamma$ phase was incorrect. Our neutron-diffraction data provide a much more robust method of studying the behavior of the key oxygen atom displacements, as compared to the previous x-ray studies. In particular, the present data highlight clearly the persistence of the $R_4^+$ octahedral tilt mode throughout the $\gamma$ phase, confirming that this phase cannot be cubic. Nevertheless, the $\gamma$ phase displays *metrically* cubic symmetry throughout its stability regime, making competing models in space groups $I4/mcm$, $Imma$, and $R\bar{3}c$ difficult to distinguish. $R\bar{3}c$ is suggested as the simplest and most physically reasonable model. The observation of clear octahedral tilts distortions in a metrically cubic perovskite is unusual but not unprecedented,[28,29] and this merits further study by techniques more sensitive to local structural effects.

## ACKNOWLEDGMENTS

The authors thank the Engineering and Physical Sciences Research Council and Science and Technology Facilities Council for funding.

*pl@st-andrews.ac.uk

[1] D. C. Arnold, K. S. Knight, F. D. Morrison, and P. Lightfoot, Phys. Rev. Lett. **102**, 027602 (2009).
[2] D. C. Arnold, K. S. Knight, G. Catalan, S. A. T. Redfern, J. F. Scott, P. Lightfoot, and F. D. Morrison, Adv. Funct. Mater. **20**, 2116 (2010).
[3] I. Sosnowska, R. Przeniosło, A. Palewicz, D. Wardecki, and A. Fitch, J. Phys. Soc. Jpn. **81**, 044604 (2012).
[4] H. Wang, C. Yang, J. Lu, M. Wu, J. Su, K. Li, J. Zhang, G. Li, T. Jin, T. Kamiyama, F. Liao, J. Lin, and Y. Wu, Inorg. Chem. **52**, 2388 (2013).
[5] J. R. Sahu and C. N. R. Rao, Solid State Sci. **9**, 950 (2007).
[6] I. H. Ismailzade, R. M. Ismailov, A. I. Alekberov, and F. M. Salaev, Phys. Status Solidi A **68**, K81 (1981).
[7] X. Qi, J. Dho, R. Tomov, M. G. Blamire, and J. L. MacManus-Driscoll, Appl. Phys. Lett. **86**, 062903 (2005).
[8] C.-H. Yang, T. Y. Koo, and Y. H. Jeong, Solid State Commun. **134**, 299 (2005).
[9] D. Kothari, V. R. Reddy, A. Gupta, D. M. Phase, N. Lakshmi, S. K. Deshpande, and A. M. Awasthi, J. Phys.: Condens. Matter **19**, 136202 (2007).
[10] S. M. Selbach, T. Tybell, M.-A. Einarsrud, and T. Grande, Chem. Mater. **21**, 5176 (2009).
[11] S. M. Selbach, T. Tybell, M.-A. Einarsrud, and T. Grande, Phys. Rev. B **79**, 214113 (2009).
[12] M. Azuma, H. Kanda, A. A. Belik, Y. Shimakawa, and M. Takano, J. Magn. Magn. Mater. **310**, 1177 (2007).

[13] A. A. Belik, A. M. Abakumov, A. A. Tsirlin, J. Hadermann, J. Kim, G. Van Tendeloo, and E. Takayama-Muromachi, Chem. Mater. **23**, 4505 (2011).
[14] S. A. T. Redfern, J. N. Walsh, S. M. Clark, G. Catalan, and J. F. Scott, arXiv:0901.3748.
[15] A. C. Larson and R. B. Von Dreele, Los Alamos National Laboratory Report LAUR 86-748, 2000 (unpublished).
[16] I. Sosnowska, W. Schäfer, and I. O. Troyanchuk, Phys. B **276–278**, 576 (2000).
[17] See Supplemental Material at http://link.aps.org/supplemental/10.1103/PhysRevB.87.224109.
[18] I. Sosnowska, W. Schäfer, W. Kockelmann, K. H. Andersen, and I. O. Troyanchuk, Appl. Phys. A **74**, S1040 (2002).
[19] A. M. Glazer, Acta Crystallogr. A **31**, 756 (1975).
[20] C. J. Howard, R. L. Withers, K. S. Knight, and Z. Zhang, J. Phys.: Condens. Matter **20**, 135202 (2008).
[21] C. J. Howard and H. T. Stokes, Acta Crystallogr. B **54**, 782 (1998).
[22] H. T. Stokes, E. H. Kisi, D. M. Hatch, and C. J. Howard, Acta Crystallogr. B **58**, 934 (2002).
[23] S. M. Selbach, M.-A. Einarsrud, and T. Grande, Chem. Mater. **21**, 169 (2009).
[24] C. J. Howard and B. J. Kennedy, J. Phys.: Condens. Matter **11**, 3229 (1999).
[25] K. S. Knight, J. Solid State Chem. **194**, 286 (2012).
[26] B. J. Kennedy, B. A. Hunter, and J. R. Hester, Phys. Rev. B **65**, 224103 (2002).
[27] B. J. Kennedy, C. J. Howard, and B. C. Chakoumakos, J. Phys.: Condens. Matter **11**, 1479 (1999).
[28] B. J. Maier, R. J. Angel, W. G. Marshall, B. Mihailova, C. Paulmann, J. M. Engel, M. Gospodinov, A.-M. Welsch, D. Petrova, and U. Bismayer, Acta Crystallogr. B **66**, 280 (2010).
[29] B. J. Maier, R. J. Angel, B. Mihailova, W. G. Marshall, M. Gospodinov, and U. Bismayer, J. Phys.: Condens. Matter **23**, 035902 (2011).